Development of the Caliper System for a Geometry PIG Based on Magnetic Field Analysis

Dong Kyu Kim*, Sung Ho Cho, Seoung Soo Park, Hui Ryong Yoo, Yong Woo Rho, Young Tai Kho

R&D Division, Korea Gas Corporation (KOGAS)
638-1, Il-dong, Ansan 425-150, Korea

Gwan Soo Park

Department of Electrical Engineering, Pusan National University, Jangjeon-dong, Geumjeong-gu, Busan 609-735, Korea

Sang Ho Park

Department of Electrical Engineering, Korea Maritime University, Youngdo-ku, Busan 606-791, Korea

This paper introduces the development of the caliper system for a geometry PIG (Pipeline Inspection Gauge). The objective of the caliper system is to detect and measure dents, wrinkles, and ovalities affect the pipe structural integrity. The developed caliper system consists of a finger arm, an anisotropic permanent magnet, a back yoke, pins, pinholes and a linear hall effect sensor. The angle displacement of the finger arm is measured by the change of the magnetic field in sensing module. Therefore the sensitivity of the caliper system mainly depends on the magnitude of the magnetic field inside the sensing module. In this research, the ring shaped anisotropic permanent magnet and linear hall effect sensors were used to produce and measure the magnetic field. The structure of the permanent magnet, the back yoke and pinhole positions were optimized that the magnitude of the magnetic field range between a high of 0.1020 Tesla and a low of zero by using three dimensional nonlinear finite element methods. A simulator was fabricated to prove the effectiveness of the developed caliper system and the computational scheme using the finite element method. The experimental results show that the developed caliper system is quite efficient for the geometry PIG with good performance.

Key Words: Caliper System, Geometry PIG, Anisotropic Permanent Magnet, FEM (Finite Element Method), Linear Hall Effect Sensor

Nomenclature

A : Magnetic vector potential [wb/m]
H_{max} : Maximum of magnetic field intensity in inside of magnet [A/m]
M : Magnetization [A/m]
L : Length of finger arm [mm]
D : Radius of wheel [m]
S_D : Size of dent [mm]
J : Current density [A/m^2]

Greeks

μ_0 : Permeability at vacuum [wb/Am]
χ : Susceptibility [A/m]

* Corresponding Author,
E-mail : giberdong@kogas.re.kr
TEL : +82-31-400-7474; **FAX** : +82-31-416-9014
R&D Division, Korea Gas Corporation (KOGAS) 638-1, Il-dong, Ansan 425-150, Korea. (Manuscript **Received** March 2, 2002; **Revised** September 27, 2003)

1. Introduction

Geometry PIG (Pipeline Inspection Gauge) is designed to provide information such as dents, ovalities, bend radius and angle, and occasionally indications of significant internal corrosion, by making measurement of the inside surface of pipeline. It is widely used during the commissioning

process of new systems and during regular maintenance of operating pipelines (Cordell and Vanzant, 1999). After commissioning, it is used most frequently before in-line inspection like as MFL (Magnetic Flux Leakage) pigging to ensure that the inspection tool can pass safely through the pipeline And it is also used for mapping and location of pipeline lately. So it must be equipped with the caliper system, odometers, IMU (Inertial Measurement Unit), tracking transmitter and large size of data acquisition and storage system. Because a geometry PIG rapidly travels through a natural gas pipeline which has so many valves, bends and tees and the inside of the pipeline are high pressure, many kinds of vibration and collision at the valve gate and tees is able to cause damage to the caliper system. So the caliper system is required to be robust to the collision and vibration and has a rapid response property. Sonar rings or mechanical fingers have been using in use until quite recently as a caliper system for geometry PIG. The caliper system using sonar ring can be adopted only in case internal fluid is liquid. So it is better suited to liquid lines and cannot be used to gas lines without liquid couplant (Tiratsoo, 1992). Therefore so many pipeline inspection service companies are using the mechanical finger system more often than sonar ring. The number of finger arms mounted on the PIG body increases as to diameter of pipe for the more coverage of circumference of pipe wall. Two types of caliper system using mechanical finger are widely used. The one is to record signal of only one displacement sensor such as LVDT (Linear Variable Differential Transformer) or potentiometer moving in accordance with the wobble plate to translate the movements of each finger and compensate for movements of PIG body. And the other is to locate rotational sensors at each finger arm and measure rotation angle of finger arm varies with the change of pipe wall geometry. The former has disadvantage to measure only the change of pipe radius. The later is required rotational sensor units as optical encoder, RVDT (Rotating Variable Differential Transformer) or potentiometer. But these rotational sensor have several problems with regard to resolution, robustness against to the collision and vibration and power consumption. So it is necessary to develop caliper system which has high resolution, low power consumption and rapid response property considering PIG running speed. In this paper, we resolved the problem by developing non-contact rotational sensor based on the principle that magnetic field in the inside of ring shaped anisotropic magnet is uniform and its tilted-angle can be measured using a linear hall effect sensor located in the inside of the permanent magnet. Because the sensitivity of the caliper system mainly depends on the magnetic field of the permanent magnet it is needed to optimize the magnetic field in the inside of the magnet. So in this paper, the structure which is composed of the permanent magnet, back yoke and pin-hole positions are optimized. And three dimensional nonlinear finite element method is used to analyze the magnetic field and to design optimally. The reliability of the developed caliper system was verified by experimental results. The experiment was fulfilled in the simulator which described the behavior of the caliper system similarly when the PIG passed through interior to the pipeline.

2. Hardware Structure and Measurement Principle

2.1 Hardware structure of geometry PIG

Geometry PIG developed in this study is composed of driving cups made of urethane, calipers, odometers, IMU (Inertial Measurement Unit), tracking transmitter and storage system for acquiring large size data as shown in Fig. 1 (Kim et

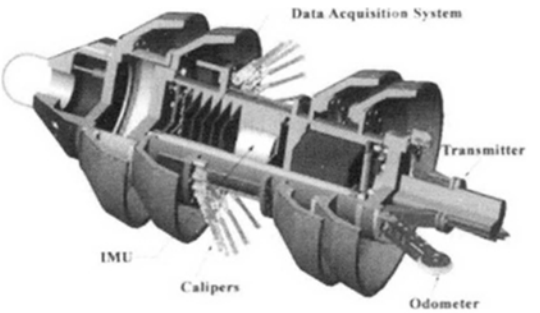

Fig. 1 Scheme of a geometry PIG

al., 2003).

Figure 2 shows the profile of developed geometry PIG. It has 24 mechanical finger arms as caliper system. And they are mounted on the PIG body at an interval of 15 degrees.

The wheel rolls along surface of pipe wall to make no scratch as shown in Fig. 3. Dents and several types of anomalies in pipeline geometry cause rotation displacement. By measuring rotation angle the size and length of dents can be determined. To measure not only the change of pipe internal radius but also bend radius and angle, ovality, we have to locate rotational sensor at rotation axis of each mechanical finger. And this requires new type of non-contact rotation sensor which has high resolution, low power consumption and rapid response property considering PIG running speed.

Fig. 2 Profile of developed geometry PIG

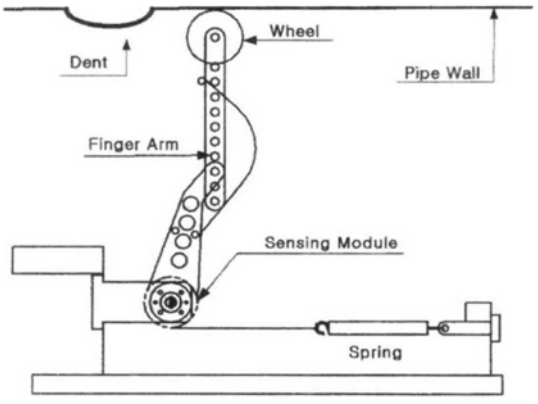

Fig. 3 Schematic diagram of the mechanical finger

2.2 Measurement principle of non-contact rotation sensor

Magnetic field in the inside of ring shaped permanent magnet magnetized like as Fig. 4 is uniform; this is shown in Fig. 5. The figure illustrates the magnitude and the direction in the center of the magnet computed by three dimensional nonlinear finite element method. The output of hall sensor signal depends on tilted angle between

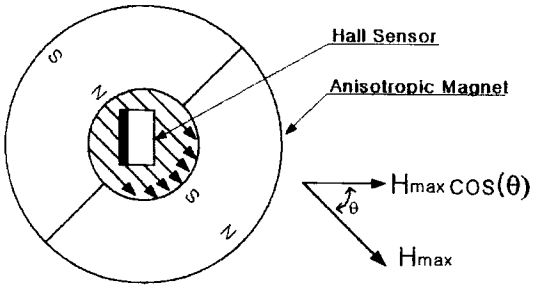

Fig. 4 Measurement principle of rotation angle

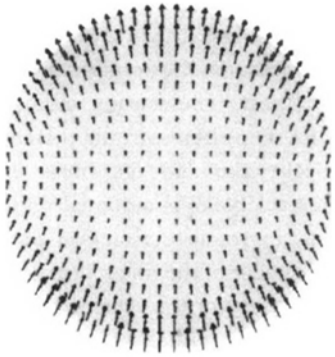

Fig. 5 Magnetic field in the inside of the ring shaped anisotropic magnet

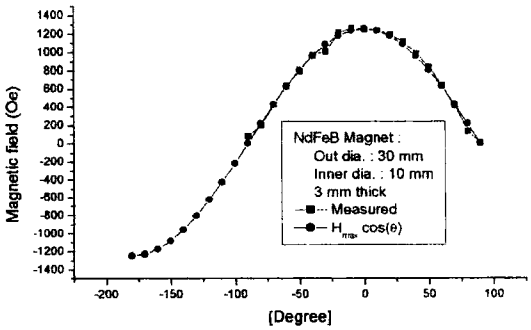

Fig. 6 Comparison between Hall sensor output and $H_{max}\cos(\theta)$ according to tilted angle change

the hall sensor plane normal and inner field of anisotropic magnet, i.e., the output of the hall sensor is $H_{max}\cos(\theta)$ where H_{max} is maximum of magnetic field intensity in inside of the magnet.

The comparison between hall sensor output and $H_{max}\cos(\theta)$ according to tilted angle change is shown in Fig. 6.

The operation of mechanical fingers ranges between a high of 90 degree and a low of zero degree and the sensitivity of the most sensitive the hall sensor now in use is 5 mV/G. Therefore it is suitable for considering input range of A/D converter that the maximum of flux density in inside of the magnet is about 0.1 Tesla. To achieve these objective, the back yoke and pin-hole positions should be optimized.

3. Magnetic Field Analysis by 3 Dimensional Nonlinear FEM and Optimum Design

Figure 7 shows the structure of the sensing module which measures the rotational angle of the mechanical finger. The sensing module is composed of ring shaped anisotropic permanent magnet, the back-yoke and the linear hall effect sensor. The back-yoke is mounted on the caliper system so as to rotate the magnet according to angle displacement of the finger arm. In this structure, the sensitivity of the sensing system mainly depends on the magnitude of the magnetic field because the sensing signals are proportional to the magnitude of the magnetic field. There could be lots of magnetic noise in measuring situation, so high SNR (signals to noise ratio) is necessary to measure the displacement of the finger arm sensitively. To increase the S/N ratio, the magnetic fields inside the sensing module are analyzed by three dimensional nonlinear finite element method and optimum size of the inner diameter, outer diameter, thickness, pinhole position of the magnet and back-yoke structures are determined. To resolve three dimensional nonlinear finite element problem, a commercial software, opera 3D was used in this research.

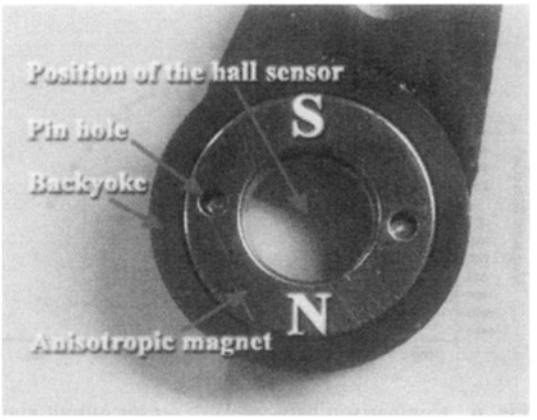

Fig. 7 Structure of the sensing module

3.1 Governing equation

The magnetic field generated by anisotropic permanent magnet is analyzed by FEM (Finite Element Method) (Park et al., 2001). In permanent the magnet system, Maxwell equations would be as follows.

$$\nabla\times H=J \tag{1}$$

$$B=\mu_0(H+M') \tag{2}$$

$$B=\nabla\times A \tag{3}$$

where B is magnetic flux density, H magnetic field intensity, J current density, A magnetic vector potential and μ_0 is magnetic permeability. In case the hysteresis of the permanent magnet could be neglected, the magnetization is conventionally represented as in eq. (4).

$$M'=\chi H \tag{4}$$

In this work, the main source of the magnetic field of the sensing system is the permanent magnet so the magnetization M' is represented by the sum of reversible component (χH) and irreversible component (M) so as to include the magnetic hysteresis of the magnet.

$$M'=\chi H+M \tag{5}$$

The magnetic field in this case is represented as follows from eqs. (5) and (2),

$$H=\nu B-\nu_r M \tag{6}$$

where $\nu=1/\mu$, $\mu=\mu_0\mu_r$, $\nu_r=1/\mu_r$ and $\mu_r=1+\chi$.

From substituting these equations into eq (1),

$$\nabla\times(\nu\nabla\times A)=J+\nu_r\nabla\times M \tag{7}$$

By the vector relations and coulomb's gauge condition, governing equation is taken as follows.

$$-(\nabla\cdot\nu\nabla)A=J+\nu_r\nabla\times M \tag{8}$$

In eqs. (8) and (3), magnetic field B could be computed by current J and magnetization M of the permanent magnet.

3.2 Formulation of finite element

In finite element analysis, the analyzing domain is divided into finite elements and fixed or free boundaries. Weighting function W is defined which satisfies the fixed boundary conditions.

Multiplying eq. (8) by weighting function and integrating in all analysis domain gives

$$\int_\Omega W\{(\nabla\cdot\nu\nabla)A+J+\nu_r\nabla\times M\}d\Omega=0 \tag{9}$$

From Green's theorem and the boundary condition, eq. (9) becomes

$$\int_\Omega\{-\nu\nabla W\nabla\cdot A+WJ-\nu_r\nabla W\times M\}d\Omega=0 \tag{10}$$

To apply the energy minima criteria, the magnetic vector potential can be calculated from eq. (10).

3.3 Magnetic field analysis by 3 dimensional nonlinear FEM and optimum design

In this sensing module, the thickness of the magnet is thin and the polarity of the magnet is not symmetry, the three dimensional analysis is inevitable. The number of elements and nodes in three dimensional analysis are approximately 200,000 and 400,000 respectively.

3.3.1 Effects of the magnetic back-yoke

Owing to the structure of the finger arm, the magnetic field of the permanent magnet is affected by the back-yoke. When the magnet is installed with or without the back-yoke, the strength of the magnetic field is computed by nonlinear FEM. The arrows represent the direction and strength of the magnetic field. As can be seen in Fig. 8 respectively, the strength of the magnetic field in

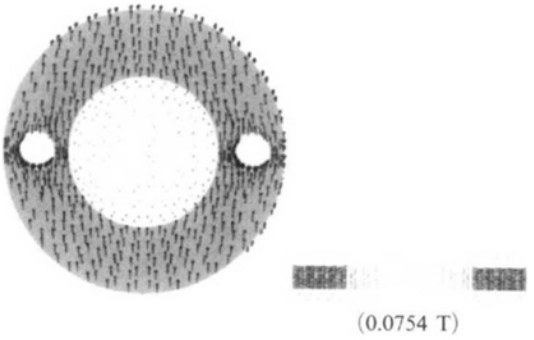

(a) Magnetic field without back-yoke

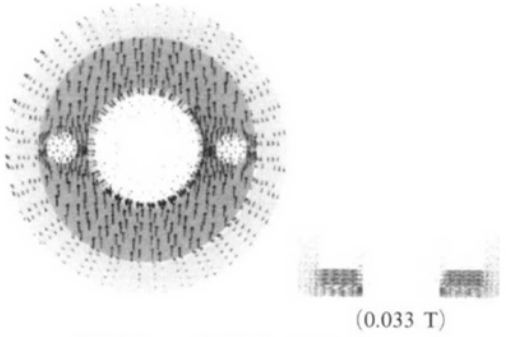

(b) Magnetic field with back-yoke

Fig. 8 Effects of the back-yoke

inside of the magnet is decreased to half when the magnet is mounted on the back-yoke. The reason is that the magnetic field produced in the permanent magnet is not maintained to the center of the ring magnet where the hall sensor is located, but returned to the back-yoke.

3.3.2 Effects of the magnet size

In order to increase the magnetic field acts on the hall sensor, outer diameter of the magnet must be increased because the inner diameter of the magnet is fixed in 16 mm. Figure 9 shows the relation between the magnetic flux density and the size of outer diameter of the magnet. The magnetic field in the hall sensor position decreases with increasing the outer diameter. The reason is considered to be large demagnetization field because of the structure and polarity of the magnet.

3.3.3 Effects of the magnet position

Although the magnetic field is decreased be-

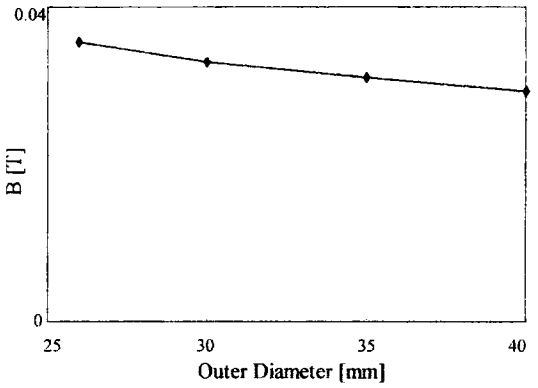

Fig. 9 Effects of the magnet size

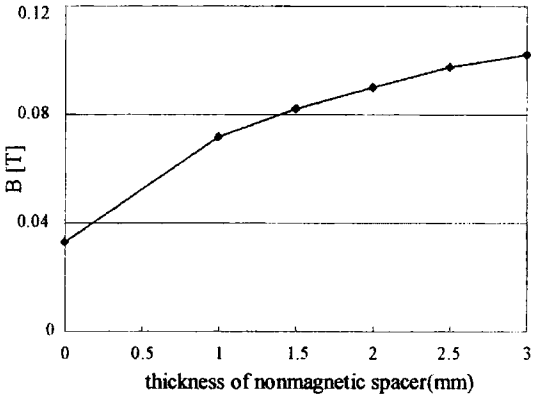

Fig. 10 Effects of the magnet position

cause of the back-yoke as in subsection 3.3.1, the back-yoke is inevitable to fabricate the finger arm. So, we changed the magnet position to avoid the return path of the magnetic flux. The non-magnetic spacer was installed between the back-yoke and permanent in order to increase the strength of the magnetic flux in center of the magnet. The relation between the magnetic flux density and the position of the magnet is shown in Fig. 10. The hall sensor is located in the center of the ring-shaped magnet and the magnetic field in there increases with increasing the thickness of the nonmagnetic spacer.

3.3.4 Effects of pinhole position

Because the magnetic field is affected by pinhole positions, the magnetic field change with respect to the pinhole positions is considered before the structure is designed. The magnetic

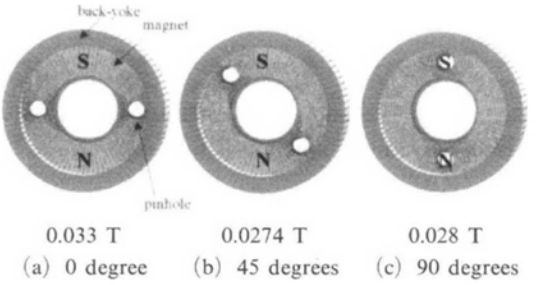

Fig. 11 Effects of the pinhole position

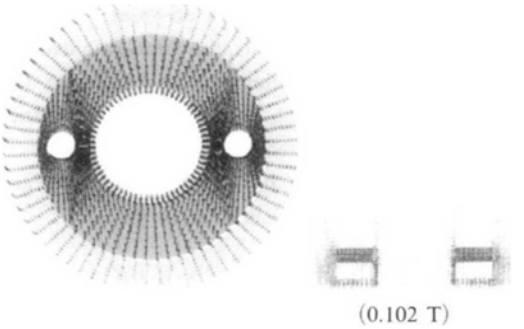

Fig. 12 Optimum design of the magnet system

field analysis based on the finite element method is performed at 0, 45 and 90 degree respectively. As can be seen in Fig. 11, the strength of the field relating pinhole positions is computed in case at 0, 45 and 90 degree respectively. With 0 degree, the magnetic field becomes maximum magnitude. Therefore, the first choice is suitable for the mechanical finger.

3.3.5 Optimum design of the finger magnet

As mentioned above, the important factors designing the mechanical finger are a presence of the magnetic back-yoke, the magnet size and the magnet pinhole positions. So that mechanical fingers are designed optimally, these factors are chosen properly. The back-yoke is inevitable owing to the structural problem of the finger. Also, pinholes are necessary components in case of the proposed mechanical finger due to the measurement principle. Ultimately, the size and the position of the magnet must be determined properly based on results of three dimensional nonlinear FEM. In this research, the maximum magnetic field in the position where the hall

sensor is installed, is increased to 0.1020 Tesla. The magnitude of the strength of the magnetic field is increased about three times in (b) of Fig. 8 as can be seen Fig. 12. As the finger rotates, the output of the hall sensor ranges from 0 to 5 Volts. This design do not need to have the electrical amplification circuit which may cause the noise and consumes the power of the system.

4. Experiment and Analysis for the Performance

The caliper system was fabricated with mentioned optimum design in section 3, as shown in Fig. 13. The output of the hall sensor whose sensitivity is 5 mV/G is 0.3~4.9 V for the angle displacement, 10-90°, which is operating range of the caliper system. We assess whether analysis results and optimum design can be adopted to the caliper system of the geometry PIG.

Figure 14 illustrates the relation between the output of the hall sensor and height change of finger wheel as rotating the finger arm. Also second order fitting equation was used for the calibration of the sensor. The geometry PIG is mounted 24 calipers at intervals of 99.1 mm, 15°, around the circumference of it. The Ch 1 and Ch 2 represent 1st caliper and 2nd calipers which were fabricated specially for the experiment in the simulator as shown in Fig. 15. The height of the finger wheel, H_D, is represented eq. (11).

$$H_D = L\sin(\theta) + D \tag{11}$$

where L is the length of the finger arm, D radius of finger wheel, θ angle the PIG body and finger arm. The dent size, S_D is determined by eq. (12) with second order fitting equation f_i as shown in Fig. 14 where i is the caliper channel.

$$S_D = f_i(V_2) - f_i(V_1) \tag{12}$$

The performance of the caliper system is estimated by the error between actual size and measured size of the dent. In order to estimate the performance, the simulator is fabricated as Fig. 15 shows.

The simulator can describe the behavior of the caliper system similarly when the PIG passes through interior to the pipeline. It mounts 2, 3, 5, 7 and 10 mm dent respectively to carry out various performance test. Fig. 16 and Table 1 show

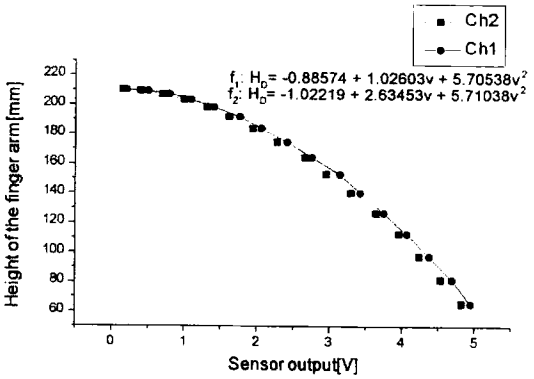

Fig. 14 Relations between sensor output and height of the wheel

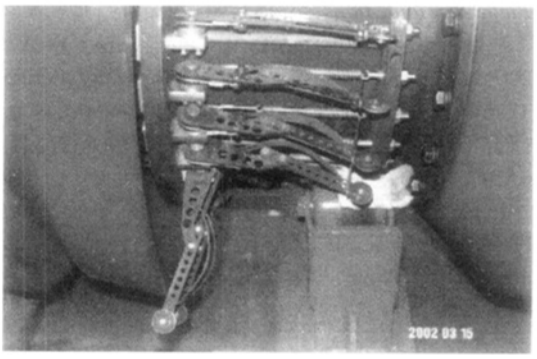

Fig. 13 Developed caliper system

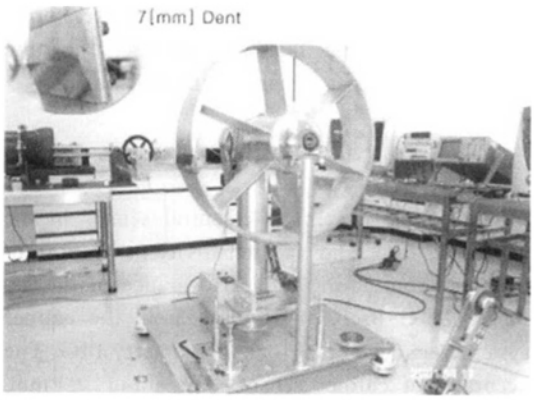

Fig. 15 Simulator for estimating the performance of the caliper system

Table 1 Experimental results and errors

Dent Sizes (mm)	Measured values of Ch 1 (mm)	Error (mm)	Measured values of Ch 2 (mm)	Error (mm)
2	2.1099	+0.10	2.3881	+0.38
3	3.1988	+0.19	3.1728	+0.17
5	4.9859	−0.01	4.9359	−0.06
7	6.8244	−0.17	7.1401	+0.14
10	9.8342	−0.16	10.230	+0.223

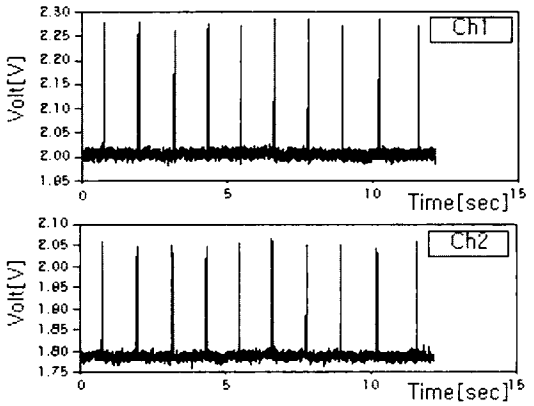

Fig. 16 Experimental results for 7 mm dent

experimental results and the error for dents. Experiment was fulfilled with constant velocity of the simulator wheel. The line velocity of the simulator wheel is about 10 m/s where it contact with the finger. Normal running speed of the PIG is about 2~4 m/s. The accuracy of the caliper system is obtained about ±1.0 mm, as shown in Table 1. It is certain that the caliper system can be used for the PIG with good performance, considering the current fact that the error of the commercial caliper system is about ±2.0 mm.

5. Conclusion

The caliper system is essential sensor in the geometry PIG and its sensitivity is important problem dominating the performance of the geometry PIG itself. In this research, the caliper system was developed for the geometry PIG. The accuracy of caliper sensors are about ±1 mm, which is more excellent than commercial sensors. It has not only high resolution but also low power consumption and rapid response property. Therefore, caliper sensors can measure features interior to the pipeline when the PIG travels at high speed. Also, three dimensional nonlinear finite element method was used to analyze the magnetic field and to design optimally, and we can be certain that computational method was quite reasonable from experimental results.

References

Cordell, J. and Vanzant, H., 1999, *All About Pigging*, On-Stream Systems Ltd and Hershel Vanzant & Associates.

Crouch, A. E., 1993, "In-Line Inspection of Natural Gas Pipelines," *Gas Research Institute Topical Report GRI 91/0365*, pp. 12~16.

Kim, D. K., Cho, S. H., Park, S. S., Yoo, H. R. and Rho, Y. W., 2003, "Design and Implementation of 30″ Geometry PIG," *KSME International Journal*, Vol. 17, No. 5, pp. 629~636.

Park, G. S., Chang, P. W. and Kim, Y. K., 2000, "Sensitive Detection of the Defect Signals in MFL Type NDT," *Proceedings of the Ninths Biennial IEEE Conference on Electromagnetic Field Computation*, pp. 181, Milwaukee, U.S.A.

Park, G. S., Chang, P. W. and Rho, Y. W., 2001, "Optimum Design of the Non-Destructive Testing System to Maximize the Magnetic Flux Leakages," *Journal of Magnetics*, Vol. 6, No. 1, pp. 31~35.

Park, G. S., Hahn, S. Y., Lee, K. S. and Jung, H. K., 1993, "Implementation of Hysteresis Characteristics using Preisach Model with M-B Variables," *IEEE Trans. Magn.*, Vol. 29 , No. 2, pp. 1542~1545.

Tiratsoo, J. N. H., 1992, *Pipeline Pigging Tech-*

nology 2nd Edition Nayler The Printer Ltd, Accrington, UK.

Todd, R. P., Ernst, H. K. and Ron, L. W., 1990, "Pipeline Geometry Pigging: Application of Strapdown INS," *IEEE Journal*, CH2811-88, pp. 353~358.